Inorg. Chem. **1989**, *28*, 2471–2475

Contribution from the Department of Chemistry,
Texas A&M University, College Station, Texas 77843

Ligand-Centered Redox Processes for MnL_3, FeL_3, and CoL_3 Complexes (L = Acetylacetonate, 8-Quinolinate, Picolinate, 2,2′-Bipyridyl, 1,10-Phenanthroline) and for Their Tetrakis(2,6-dichlorophenyl)porphinato Complexes [M(Por)]

Silvia A. Richert, Paul K. S. Tsang, and Donald T. Sawyer*

Received September 29, 1988

The potentials for the ML_3^-/ML_3 couple of MnL_3, FeL_3, and CoL_3 complexes (L = acetylacetonate, 8-quinolinate, picolinate, 2,2′-bipyridyl, 1,10-phenanthroline) occur at substantially less positive values than those for their zinc analogues and are clearly ligand-centered. The negative shift in potential for these ligand oxidations is proportional to their metal–ligand covalent-bond energies. The reductions for the bipyridyl and phenanthroline complexes of these transition metals also are ligand-centered. Electrochemical characterization of tetrakis(2,6-dichlorophenyl)porphine and of its neutral porphinato complexes with Zn, Mn, Fe, and Co indicates that electron transfer occurs within the porphyrin ring and that the metal–porphyrin bonding involves covalent σ bonds between d^nsp valence electrons of the neutral metal (or hydrogen atoms of porphine) and two pyrrole p electrons of the uncharged porphyrin.

Several electrochemical investigations of transition-metal complexes have presented evidence that the electron transfer is ligand-centered rather than metal-centered. Thus, the oxidations of metal–catecholate,[1-3] metal–dithiolate,[4] and metal-hydroxide[5] complexes are facilitated by stabilization of the ligand-radical product via covalent-bond formation with an unpaired d electron of the transition-metal center. The negative shift in the potential for ligand oxidation relative to that for the free ligand anion is proportional to this covalent-bond energy.

In a recent study[6] the electron-transfer chemistry for a variety of manganese complexes has been characterized to be ligand-centered for all cases. This result has prompted us to extend the investigation to a parallel series of iron and cobalt complexes. The goal has been to establish that ligand-centered oxidations in transition-metal complexes are general and that the oxidation potential ($E^{\circ\prime}_{ML_3/ML_3^-}$) for the complex is determined by the relation

$$E^{\circ\prime}_{ML_3/ML_3^-} = E^{\circ\prime}_{L^\cdot/L^-} + (-\Delta G)_{BF}/23.1\ \text{kcal V}^{-1} \qquad (1)$$

where $(-\Delta G)_{BF}$ is the free energy of formation for the L_2M–L covalent bond ($L_2M^\cdot + {}^\cdot L$).

Experimental Section

Equipment. Cyclic voltammetry was accomplished with a Bioanalytical Systems Model CV-27 voltammetric controller and a Houston Instruments Model 200 XY recorder. The electrochemical measurements were made with a 15-mL microcell assembly that included a Bioanalytical Systems glassy-carbon inlay electrode (area 0.09 cm^2), a platinum-wire auxiliary electrode, and a Ag/AgCl reference electrode (filled with aqueous tetramethylammonium chloride solution and adjusted to 0.00 V vs SCE) with a solution junction via a Pyrex tube with a soft-glass cracked tip.[7] The reference electrode was contained in a luggin capillary, and the auxiliary electrode was contained in a glass tube with a medium-porosity glass frit and filled with a concentrated solution of supporting electrolyte. The UV-visible spectra were obtained with a Hewlett-Packard Model 8450A diode-array spectrophotometer. Magnetic susceptibilities of the complexes in solution were measured by the Evans method[8-10] on a Varian VL-200 NMR spectrometer. Elemental analysis was performed by Galbraith Laboratories, Inc.

Chemicals and Reagents. The reagents for the investigations and syntheses were the highest purity commercially available and were used without further purification. $Mn(acac)_3$ (McKenzie) was recrystallized from benzene before use, and $Fe(acac)_3$ (McKenzie) was recrystallized from acetonitrile. Burdick and Jackson "distilled in glass" grade dimethylformamide (DMF), acetonitrile (MeCN), and methylene chloride (CH_2Cl_2) were used without further purification as the solvents for the electrochemical experiments. High-purity argon gas was used to deaerate the solutions. The complexes were dried in vacuo over $CaSO_4$ for 24 h prior to use in electrochemical or magnetic measurements.

Syntheses of Complexes. Several complexes were prepared by conventional methods: $Mn(PA)_3 \cdot H_2O$,[11-13] $Mn(8Q)_3$,[12] $Mn(bpy)_3(ClO_4)_2$,[13] $Mn(phen)_3(ClO_4)_2$,[13-15] $Mn(OPPh_3)_4(ClO_4)_2$,[16] $Fe(8Q)_3$,[17] $Fe(OPPh_3)_4(ClO_4)_2$,[18] $Na_3[Co(CO_3)_3] \cdot 3H_2O$,[19] $Co(acac)_3$,[20] $Co(bpy)_3(ClO_4)_2$,[21] $Co(phen)_3(ClO_4)_2$,[14] $Co(OPPh_3)_4(ClO_4)_2$,[16] and $Zn(bpy)_3(ClO_4)_2$[13] (acacH = acetylacetone; 8QH = 8-quinolinol; PAH = picolinic acid; bpy = 2,2′-bipyridyl; phen = 1,10-phenanthroline; $OPPh_3$ = triphenylphosphine oxide).

$M(MeCN)_4(ClO_4)_2$. The $M(MeCN)_4(ClO_4)_2$ complexes of Mn, Fe, and Co were prepared by multiple recrystallizations of the commercial hydrated perchlorates in dry MeCN.

Ligand Anion Solutions. Solutions of $acac^-$, $8Q^-$, and PA^- were prepared by mixing the appropriate ligand (acacH, 8QH, PAH) with $(Bu_4N)OH$ (1 M tetrabutylammonium hydroxide in methanol; Aldrich).

$Fe(PA)_3$. A 1 mM solution of this complex was prepared in situ by mixing $Fe(ClO_4)_3$ (anhydrous, Strem) with 3 equiv of PA^-.

$Co(PA)_3$ and $Co(8Q)_3$. These complexes were prepared by a variation of a literature method for the synthesis of $Co(acac)_3$.[20] A 3-equiv amount of ligand (approximately 4 g) in 150 mL of solvent was mixed with $Na_3[(Co(CO_3)_3] \cdot 3H_2O$ in the presence of 2 mL of 70% $HClO_4$. $Co(PA)_3$ was prepared in water, while the synthesis of $Co(8Q)_3$ was carried out in 95% ethanol. The products were recrystallized from water, then heptane, and absolute ethanol, respectively. Purple crystals were obtained for $Co(PA)_3$ (λ_{max} 376, 528 nm). Anal. Calcd for $CoC_{18}H_{12}N_3O_6$: C, 50.84; H, 2.84; N, 9.88; O, 22.57; Co, 13.86. Found: C, 50.78; H, 2.84; N, 9.76; O, 23.05; Co, 13.77.

$(Cl_8TPP)M(ClO_4)$. 5,10,15,20-Tetrakis(2,6-dichlorophenyl)porphine (Cl_8TPPH_2) was synthesized from 2,4,6-collidine[22,23] and was used to

---

(1) Jones, S. E.; Leon, L. E.; Sawyer, D. T. *Inorg. Chem.* **1982**, *21*, 3692–3698.

(2) Bodini, M. E.; Copia, G.; Robinson, R.; Sawyer, D. T. *Inorg. Chem.* **1983**, *22*, 126–129.

(3) Haga, M.-A.; Radsworth, E. S.; Lever, A. B. P. *Inorg. Chem.* **1986**, *25*, 447–453.

(4) Sawyer, D. T.; Srivatsa, G. S.; Bodini, M. E.; Schaefer, W. P.; Wing, R. M. *J. Am. Chem. Soc.* **1986**, *108*, 936.

(5) Tsang, P. K. S.; Cofré, P.; Sawyer, D. T. *Inorg. Chem.* **1987**, *26*, 3604.

(6) Richert, S. A.; Tsang, P. K. S.; Sawyer, D. T. *Inorg. Chem.* **1988**, *27*, 1814.

(7) Sawyer, D. T.; Roberts, J. L., Jr. *Experimental Electrochemistry for Chemists*; Wiley-Interscience: New York, 1974; pp 44–46, 144–145, 336–339.

(8) Evans, D. F. *J. Chem. Soc.* **1959**, 2003.

(9) Carlin, R. L. *Magnetochemistry*; Springer-Verlag: New York, 1986.

(10) Brevard, C.; Granger, P. *Handbook of High Resolution Multinuclear NMR*; Wiley-Interscience: New York, 1981.

(11) Yamaguchi, K.; Sawyer, D. T. *Inorg. Chem.* **1985**, *24*, 971.

(12) Summers, J. Ph.D. Dissertation, University of Michigan, 1968; available from University Microfilms International, Ann Arbor, MI.

(13) Morrison, M. M.; Sawyer, D. T. *Inorg. Chem.* **1978**, *17*, 333.

(14) Schilt, A. A.; Taylor, R. C. *J. Inorg. Nucl. Chem.* **1959**, *9*, 211.

(15) Chiswell, B.; O'Reilly, E. J. *Inorg. Chim. Acta* **1973**, *7*, 707.

(16) Bannister, E.; Cotton, F. A. *J. Chem. Soc.* **1960**, 1878.

(17) Furman, N. H. *Standard Methods of Chemical Analysis*, 6th ed.; D. Van Nostrand, Inc: Princeton, NJ, 1962; Vol. 1, pp 537–538.

(18) Karayannis, N. M.; Mikulski, C. M.; Strocko, M. J.; Pytlewski, L. L.; Labes, M. M. *J. Inorg. Nucl. Chem.* **1970**, *32*, 2629.

(19) Bauer, H. F.; Drinkard, W. C. *J. Am. Chem. Soc.* **1960**, *82*, 5031.

(20) Bryant, B. E.; Fernelius, W. C. In *Inorganic Synthesis V*; Moeller, T., Ed.; McGraw-Hill: New York, 1957; pp 188–189.

(21) Wheeler, S. H.; Zingheim, S. C.; Nathan, L. C. *J. Inorg. Nucl. Chem.* **1978**, *40*, 779.

0020-1669/89/1328-2471$01.50/0

Table I. Oxidation Potentials for Ligand Anions and Their Complexes with Manganese, Iron, and Cobalt in Acetonitrile (0.1 M Tetraethylammonium Perchlorate)

	$E_{1/2}$,[b] V vs SCE[c]				
lig anion (L^-)[a]	$L^-/L^\bullet$	$ZnL_3^-/ZnL_2(L^\bullet)$	$MnL_3^-/Mn(^\bullet L)L_2/[(Mn(^\bullet L)_2L^+)]$	$FeL_3^-/Fe(^\bullet L)L_2$	$CoL_3^-/Co(^\bullet L)L_2$
$8Q^-$	−0.03	−0.02	−0.30 (+0.73)	−0.65[d]	−0.71[d]
$acac^-$	+0.31	+0.34	−0.06 (+0.96)	−0.66	−0.59
PA^-	+1.26	+1.30	+0.36 (+1.35)	−0.04	−0.20
$M^{2+}/M^{3+}(H_2O, pH\ 0)$[e]			+1.27 (>+2.30)[f]	+0.53 (+1.60)[g]	+1.68 (>+2.30)[h]

[a] Key: $8Q^-$, 8-quinolinate; $acac^-$, acetylacetonate; PA^-, picolinate. [b] $E_{1/2}$ taken as $(E_{p,a} + E_{p,c})/2$ for reversible couples of Mn and Fe complexes; as $E_{p,a/2} + 0.03$ V for L^- and ZnL_3^-, and as $E_{p,c/2} - 0.03$ V for Co complexes that exhibit separated redox couples; ref 27. [c] Saturated calomel electrode (SCE) vs NHE, +0.242 V. [d] Solubility in MeCN: $Fe(8Q)_3$, <1 mM; $Co(8Q)_3$, <0.5 mM. [e] Standard reduction potentials, ref 28. [f] $[Mn(MeCN)_4](ClO_4)_2$ in MeCN. [g] $[Fe(MeCN)_4](ClO_4)_2$ in MeCN. [h] $[Co(MeCN)_4](ClO_4)_2$ in MeCN.

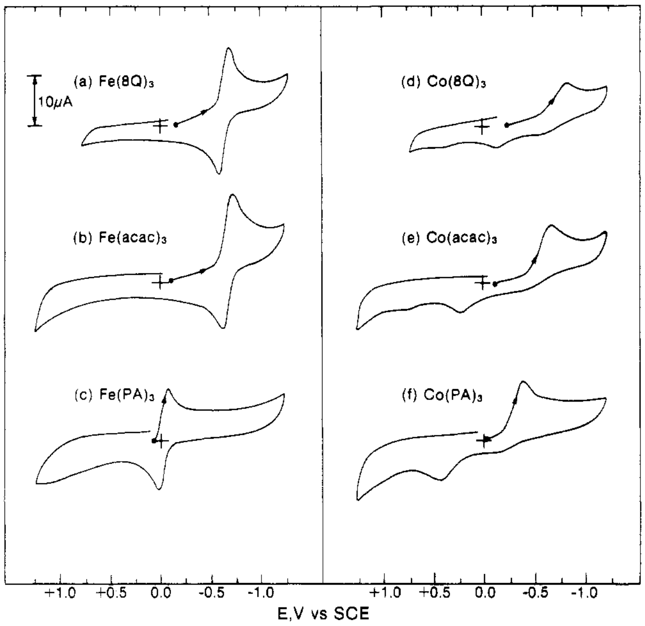

Figure 1. Cyclic voltammograms of 1 mM solutions in DMF [0.1 M $(Et_4N)ClO_4$]: (a) $Fe(8Q)_3$; (b) $Fe(acac)_3$; (c) $Fe(PA)_3$; (d) $Co(8Q)_3$, not completely soluble; (e) $Co(acac)_3$; (f) $Co(PA)_3$. Conditions: scan rate 0.1 V s^{-1}; 25 °C; glassy-carbon working electrode (0.09 cm^2); saturated calomel electrode (SCE) vs NHE, +0.242 V.

prepare $(Cl_8TPP)MnCl$,[24] $(Cl_8TPP)FeCl$,[24,25] $(Cl_8TPP)Co$,[24] and $(Cl_8TPP)Zn$.[22,23] The perchlorate salts $(Cl_8TPP)Mn(ClO_4)$ and $(Cl_8TPP)Fe(ClO_4)$ were then prepared by addition of $AgClO_4$ in toluene.[26]

Results

Figure 1 illustrates the cyclic voltammograms for the FeL_3 and CoL_3 complexes [L = 8-quinolinate ($8Q^-$), acetylacetonate ($acac^-$), picolinate (PA^-)]. The redox couples for the FeL_3 complexes are reversible, but the cyclic voltammograms for the cobalt complexes exhibit widely separated anodic and cathodic peaks. Figure 2 illustrates the cyclic voltammograms for the acetylacetonate anion ($acac^-$) and its tris complexes with manganese, iron, and cobalt. Similar voltammograms are observed for the 8-quinolinate and picolinate anions and for their metal complexes. The $E_{1/2}$ values for these anions and their metal complexes are summarized in Table I.

The electrochemistry for the MnL_3 complexes is characterized by two reversible redox couples, while that of FeL_3 exhibits one reversible couple. In contrast, the electrochemistry of CoL_3 is characterized by a widely separated irreversible couple (Figures 1 and 2). Similar electrochemistry is observed for ($CoL_2 + L^-$) and ($CoL_2 + {}^-OH$) with the peaks shifted by only a few hundreths of a volt. Addition of a second equivalent of hydroxide ion to ($CoL_2 + {}^-OH$) leads to the formation of a brown precipitate. For CoL_3, an oxidation peak is not observed for an initial anodic scan but is seen only after reduction to an anionic species.

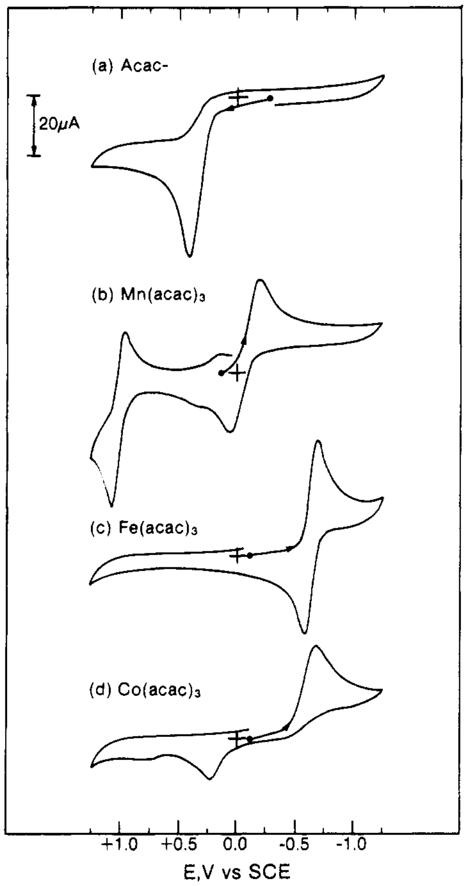

Figure 2. Cyclic voltammograms of 3 mM solutions in DMF [0.1 M $(Et_4N)ClO_4$]: (a) acetylacetonate ($acac^-$) [acacH + $(Me_4N)OH$, 1:1]; (b) $Mn(acac)_3$; (c) $Fe(acac)_3$; (d) $Co(acac)_3$. Conditions: scan rate 0.1 V s^{-1}; 25 °C; glassy-carbon working electrode (0.09 cm^2); SCE vs NHE, +0.242 V.

The solution magnetic moments (μ_B) for the cobalt and iron complexes are as follows: $Fe(8Q)_3$, 6.35; $Fe(acac)_3$, 5.88; $Co(8Q)_3$, diamagnetic; $Co(acac)_3$, 0.61 (diamagnetic); $Co(PA)_3$, 0.66 (diamagnetic).

Addition of hydroxide ion [$(Bu_4N)OH$] to a solution of $Fe(acac)_3$ results in a green color that persists for several seconds at room temperature [a broad band (600–800 nm) is observed for the absorption spectrum during the period that the green color persists]. Figure 3 illustrates that the addition of hydroxide ion causes a reduction in the peak current for $Fe(acac)_3$, the appearance of an oxidation peak at +0.02 V vs SCE, and a broad

---

(22) Traylor, P. S.; Dolphin, D.; Traylor, T. G. *J. Chem. Soc., Chem. Commun.* **1984**, 279–280.
(23) Badger, G. M.; Jones, R. A.; Laslett, R. L. *Aust. J. Chem.* **1964**, *17*, 1028.
(24) Alder, A. D.; Longo, F. R.; Varadi, V. *Inorg. Synth.* **1976**, *16*, 213–220.
(25) Kobayashi, H.; Higuchi, T.; Kaizu, Y.; Osada, H.; Aoki, M. *Bull. Chem. Soc. Jpn.* **1975**, *48*, 3137–3141.
(26) Hill, C. L.; Williamson, M. M. *Inorg. Chem.* **1985**, *24*, 2836.
(27) Bard, A. J.; Faulkner, L. R. *Electrochemical Methods*; Wiley: New York, 1980; pp 236–243.
(28) Bard, A. J.; Parsons, R.; Jordon, J. *Standard Potentials in Aqueous Solution*; Dekker: New York, 1985.

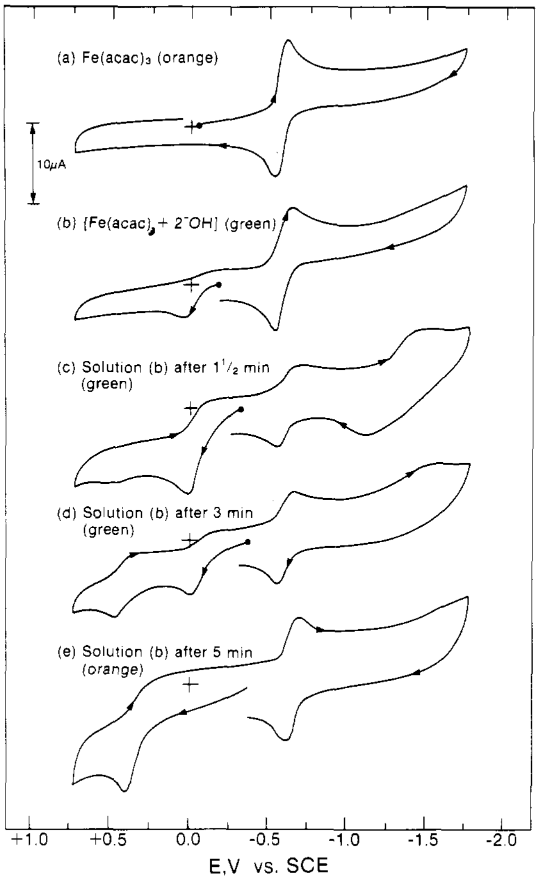

Figure 3. Cyclic voltammograms: (a) 0.5 mM $Fe(acac)_3$; (b) 0.5 mM $Fe(acac)_3$ + 2 equiv of ^-OH [$(Bu_4N)OH$], initial scan; (c) solution from (b), 1.5 min later; (d) solution from (b), 3 min later; (e) solution from (b), 5 min later. Cold MeCN [0.1 M $(Et_4Cl)ClO_4$] (dry ice/MeCN bath) solutions were used. Conditions: scan rate 0.1 V s^{-1}; glassy-carbon working electrode (0.09 cm^2); SCE vs NHE, +0.242 V.

reduction at −1.5 V. The reduction is coupled with an oxidation feature at ∼−1.14 V. With time the oxidation at +0.02 V disappears and is replaced by the oxidation peak for free $acac^-$ at +0.34 V, the broad reduction decreases, and the initial $Fe(acac)_3$ couple regains some of its amplitude.

Figure 4 illustrates the redox chemistry for 2,2′-bipyridyl (bpy) and its zinc, iron, and cobalt complexes [$Zn(bpy)_3^{2+}$, $Fe(bpy)_3^{2+}$, $Co(bpy)_3^{2+}$]. The Fe and Co complexes exhibit a reversible oxidation couple, and the Fe complex has three reversible reduction couples, while the Co complex has two reduction couples with the second a two-electron process. The $Zn(bpy)_3^{2+}$ complex is not oxidized but exhibits sharp peaks that are characteristic of metal plating and anodic stripping from the electrode surface [for $Zn(MeCN)_4(ClO_4)_2$ these peaks occur at $E_{p,c} = -1.10$ V and $E_{p,a} = -0.57$ V vs SCE]. The potentials for the redox couples of the tetrakis or tris complexes of Mn, Fe, and Co with acetonitrile, triphenylphosphine oxide, 2,2′-bipyridyl, and 1,10-phenanthroline are summarized in Table IIA. The three reversible reduction couples for the $Mn(bpy)_3^{2+}$ and $Fe(bpy)_3^{2+}$ complexes with essentially identical potentials are noteworthy [as is the first reduction for $Zn(bpy)_3^{2+}$]. Table IIB summarizes the $E_{1/2}$ values of the redox couples for the tris(bipyridyl) complexes of Zn, Mn, Fe, and Co [$M(bpy)_3^{2+}$]. The cyclic voltammograms of the tetrakis(2,6-dichlorophenyl)porphinato complexes of Zn, Mn, Fe, and Co, and of the parent porphine are illustrated in Figure 5. The $E_{1/2}$ values for the oxidation and reduction couples for these complexes are listed in Table IIC.

Discussion and Conclusions

The oxidation potentials for the ML_3^- complexes are substantially less positive by 0.27–1.46 V (Table I) than those for the free ligand anion ($L^-/L^•$), and in the case of FeL_3^- and MnL_3^- the oxidations are reversible (those for L^- are irreversible). The irreversible reduction for the CoL_3 complexes appears to be the result of the propensity of CoL_3^- anions to hydrolyze

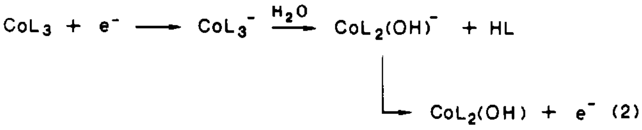
$$CoL_3 + e^- \longrightarrow CoL_3^- \xrightarrow{H_2O} CoL_2(OH)^- + HL \qquad CoL_2(OH)^- \longrightarrow CoL_2(OH) + e^- \quad (2)$$

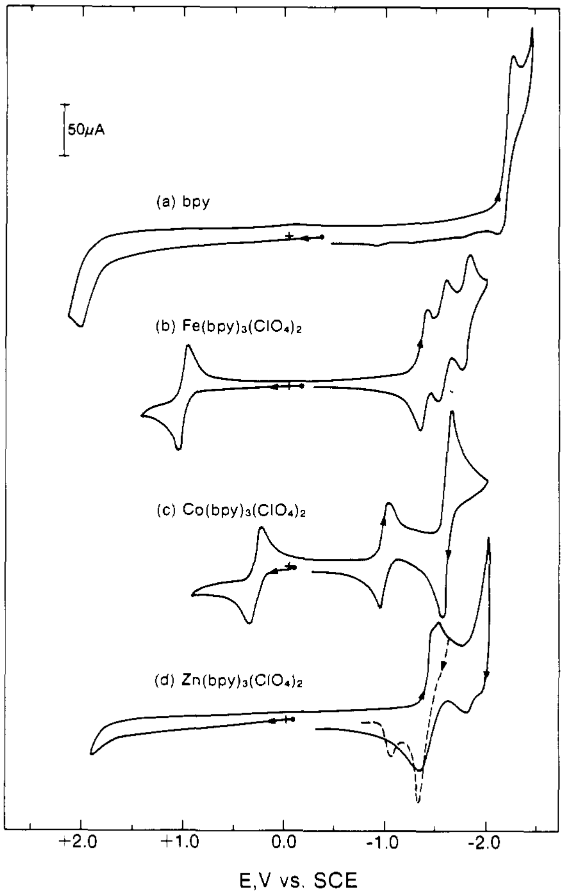

Figure 4. Cyclic voltammograms of 3 mM solutions in MeCN (0.1 M tetraethylammonium perchlorate): (a) bpy; (b) $Fe(bpy)_3^{2+}$; (c) $Co(bpy)_3^{2+}$; (d) $Zn(bpy)_3^{2+}$. Conditions: scan rate 0.1 V s^{-1}; 25 °C; glassy-carbon working electrode (0.09 cm^2); SCE vs NHE, +0.242 V.

Thus, the reoxidation is of $[CoL_2(OH)]^-$. Although these ML_3^-/ML_3 couples traditionally are attributed to M(II)/M(III) metal-centered oxidation processes, their oxidation potentials are substantially less positive than (a) those for the solvated M(II) ions or (b) those for oxidation of the free ligand anion (L^-) (Table I). This negative shift in oxidation potential also has been rationalized as due to enhanced stabilization of high-valence states. If stabilization of the M(III) state were the process, then the $M(PA)_3^-$ complexes should have the most negative (least positive) oxidation potentials [actually, they have the least negative (most positive) potentials]. Instead, the trend of oxidation potentials for the ML_3 complexes parallels that for free ligands (and their ZnL_3^- complexes).[6] Thus, the redox chemistry of iron and cobalt complexes is consistent with ligand-centered processes, as it has been shown to be for manganese complexes.[6]

The shifts in the oxidation potentials for ML_3^- complexes are consistent with oxidation of the ligand anion ($L^- \rightarrow L^•$) and its concerted stabilization by covalent-bond formation with the unpaired $d^n sp$ valence electrons of manganese (d^5sp), iron (d^6sp or d^5sp^2), and cobalt (d^7sp or d^6sp^2). The apparent free energy of covalent-bond formation, $-\Delta G_{BF}$, can be estimated from the shift in potential for $ZnL_3^-/ZnL_2(L^•)$ and ML_3^-/ML_3 oxidation processes

$$-\Delta G_{BF} = [E_{1/2[ZnL_3^-/ZnL_2(L^{•-})]} - E_{1/2(ML_3^-/M(^•L)L_2)}] \times 23.1 \text{ kcal} \quad (3)$$

where $E_{1/2}$ is taken as $(E_{p,a} + E_{p,c})/2$ for the MnL_3 and FeL_3

Table II. Redox Potentials for Mn, Fe, and Co Complexes with Neutral Ligands and Porphyrins

A. $ML_n^{2+/3+}$ Couples in MeCN

	$E°'$, V vs SCE		
	$MnL_n^{2+/3+}$	$FeL_n^{2+/3+}$	$CoL_n^{2+/3+}$
$[M(MeCN)_4](ClO_4)_2$	>+2.3	+1.61 ($d^6 \rightarrow d^5$)	>+2.3
$[M(OPPh_3)_4](ClO_4)_2$	>+2.3	+1.03	>+2.3
$[M(bpy)_3](ClO_4)_2$	+1.31	+1.06	+0.34
$[M(phen)_3](ClO_4)_2$	+1.32	+1.08	+0.38

B. Ligand-Centered Processes for $M(bpy)_3^{2+}$ Complexes in MeCN

	$E°'$, V vs SCE			
	3+/2+	2+/+	+/0	0/–
bpy	+2.08 (+/0)			–2.19
$Zn(bpy)_3^{2+}$	>+2.3	–1.37 (2e)[a]		–1.85[a]
$Mn(bpy)_3^{2+}$	+1.31	–1.36	–1.54	–1.75
$Fe(bpy)_3^{2+}$	+1.06	–1.35	–1.54	–1.78
$Co(bpy)_3^{2+}$	+0.34	–0.95	–1.57 (2e)	

C. Ligand-Centered Processes for $(Cl_8TPP)M$ Complexes in CH_2Cl_2[b]

	$E°'$, V vs SCE				
	$MP^{2+} \leftarrow MP^{\bullet+}$	$MP^{\bullet+} \leftarrow MP$	$PML \leftarrow PM + L^-$	$MP \rightarrow MP^{\bullet-}$	$MP^{\bullet-} \rightarrow MP^{2-}$
$(Cl_8TPP)H_2$	+1.63	+1.23		–1.10 (–0.90)	–1.54 (–1.32)
$(Cl_8TPP)Zn$	+1.34	+1.02 (+1.00)		–1.27 (–1.21)	–1.72 (–1.64)
$(Cl_8TPP)Mn(Cl)$[c]	+1.49	–0.06 (–0.16)	–0.23	–1.34 (–1.17)	(–1.70)
$(Cl_8TPP)Fe(Cl)$	+1.64	+1.35 (+1.20)	–0.29 (–0.14)	–0.97 (–1.00) ($M \rightarrow M^-$)	–1.63 (–1.55)
$(Cl_8TPP)Co$	+1.25	+0.82 (+0.25)		–0.86 (–0.76) ($M \rightarrow M^-$)	–1.29 (–1.79)
$(Cl_8TPP)Fe(-OH)$[d]	+1.64	+1.35	–0.75 (–0.70)	–1.31 (–1.34)	–1.63 (–1.55)

[a] Overlap of $Zn^{2+/0}$ plating onto electrode surface and reduction of complex. [b] Data in parentheses are for DMF solvent. [c] $(Cl_8TPP)Mn(-Cl) \rightarrow [(Cl_8TPP)Mn(-Cl)]^+ + e^-$, $E°' = +0.88$ V vs SCE. [d] $(Cl_8TPP)Fe(-OH) \rightarrow [(Cl_8TPP)Fe(-OH)]^+ + e^-$, $E°' = +1.00$ V vs SCE; generated from $(Cl_8TPP)FeCl$ plus 1 equiv of $(Bu_4N)OH$.

Scheme I

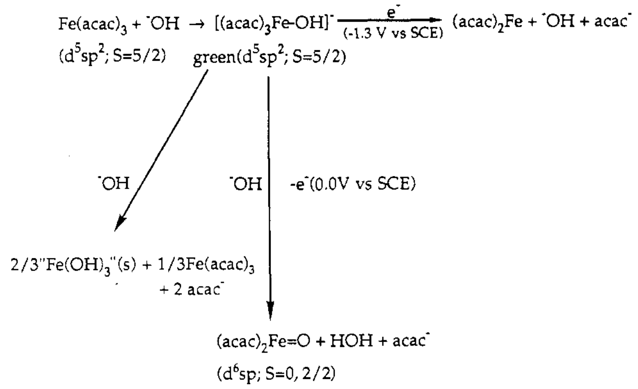

Table III. Apparent Metal–Ligand Covalent-Bond-Formation Free Energies ($-\Delta G_{BF}$) for Several Manganese, Iron, and Cobalt Complexes

complex	$-\Delta G_{BF}$, kcal[a]
A. Manganese	
$(8Q)_2Mn{-}8Q$	6
$(acac)_2Mn{-}acac$	9
$(PA)_2Mn{-}PA$	22
$(Cl_8TPP)Mn{-}OH(d^5sp)$	27[b]
$Cl_8TPP^+{-}Mn(d^5sp)$	27[c]
$[(bpy)_2Mn{-}bpy]^{3+}$	>23[c]
B. Iron	
$(8Q)_2Fe{-}8Q$	15
$(acac)_2Fe{-}acac$	23
$(PA)_2Fe{-}PA$	31
$(Cl_8TPP)Fe{-}OH(d^5sp^2)$	32[b]
$(Cl_8TPP)Fe{-}Cl(d^5sp^2)$	53
$(Cl_8TPP)Fe{=}O(d^6sp)$	66[b,d]
$[(bpy)_2Fe{-}bpy]^{3+}$	>29[c]
$[(Ph_3PO)_3Fe{-}OPPh_3]^{3+}$	>30[c]
C. Cobalt	
$(8Q)_2Co{-}8Q$	16
$(acac)_2Co{-}acac$	21
$(PA)_2Co{-}PA$	35
$(Cl_8TPP)Co{-}OH(d^7sp$ or $d^6sp^2)$	26[b]
$Cl_8TPP^+{-}Co$	17[c]
$[(bpy)_2Co{-}bpy]^{3+}$	>46[c]

[a] $-\Delta G_{BF} = [E_{1/2[ZnL_3^-/ZnL_2(L\bullet)]} - E_{1/2(ML_3^-/M(\bullet L)L_2)}] \times 23.1$ kcal. [b] $-\Delta G_{BF} = [E_{p,a(^-OH/\bullet OH)} - E_{p,a(M,^-OH/MOH)}] \times 23.1$ kcal; ref 29. [c] $-\Delta G_{BF} = [E_{p,a(ZnL/ZnL\bullet^+)} - E_{p,a(ML/M-L^+)}] \times 23.1$ kcal; L = $(bpy)_3$ or Cl_8TPP. [d] $-\Delta G_{BF}$ for π-bond, $[(Por)Fe{=}O + e^- \rightarrow (Por)Fe{-}O^-]$.

complexes, as $E_{p,a/2} + 0.03$ V for ZnL_3^-, and as $E_{p,c}/2 - 0.03$ V for CoL_3 complexes.[27] The apparent bond-formation energies for the ML_3 complexes, based on the data in Table I,[28] are given in Table III.[29] The MnL_3 complexes have bond energies weaker (by 8–13 kcal) than those for FeL_3 and CoL_3. The bond energies of metal–hydroxide for the metal porphyrins are similar.[30]

Reference to Figure 3 confirms that the addition of ^-OH to $Fe(acac)_3$ does not immediately displace an $acac^-$ ion upon formation of the green intermediate. With time the intermediate hydrolyzes to a "$Fe(OH)_3$" precipitate and the original tris complex. The green intermediate has not been isolated or structurally characterized, but a reaction sequence that is consistent with the experimental results and the bond energies of Table III is outlined in Scheme I.

With neutral ligands (Ph_3PO, bpy, phen) the redox processes for the $ML_{3,4}^{2+}$ complexes (Table II) also are consistent with ligand-centered electron transfer. As with the anionic ligands, oxidation of the free ligand occurs at much more positive potentials than it does for those associated with Mn, Fe, or Co. Because an oxidation is not observed for the zinc complex prior to the solvent edge, only a lower limit may be obtained for the apparent free energy of covalent-bond formation (Table III).

Because the three metal–ligand bonds for the ML_3^{3+} complexes of Table II are equivalent and covalent, the valence electrons for the uncharged metal centers [$Mn(d^5s^2)$, $Fe(d^6s^2)$, $Co(d^7s^2)$] must

---

(29) That this approach is sound and yields valid covalent-bond energies is confirmed by the results for the H–OH bond of water. From the standard redox potentials[28] ($E°_{^-OH/\bullet OH} = +1.89$ V vs NHE and $E°_{^-OH,H\bullet/H-OH} = -2.93$ V), eq 3 gives a $-\Delta G_{BF}$ value of 111 kcal for the H–OH bond. This is identical with the literature value ($\Delta H_{DBE} = 119$ kcal $= -\Delta G_{BF} + T\Delta S = 111 + 8$): *CRC Handbook of Chemistry and Physics*, 68th ed.; CRC: Boca Raton, FL, 1987; p F-179.

(30) Sawyer, D. T.; Chooto, P.; Tsang, P. K. S. *Langmuir* **1989**, *5*, 84.

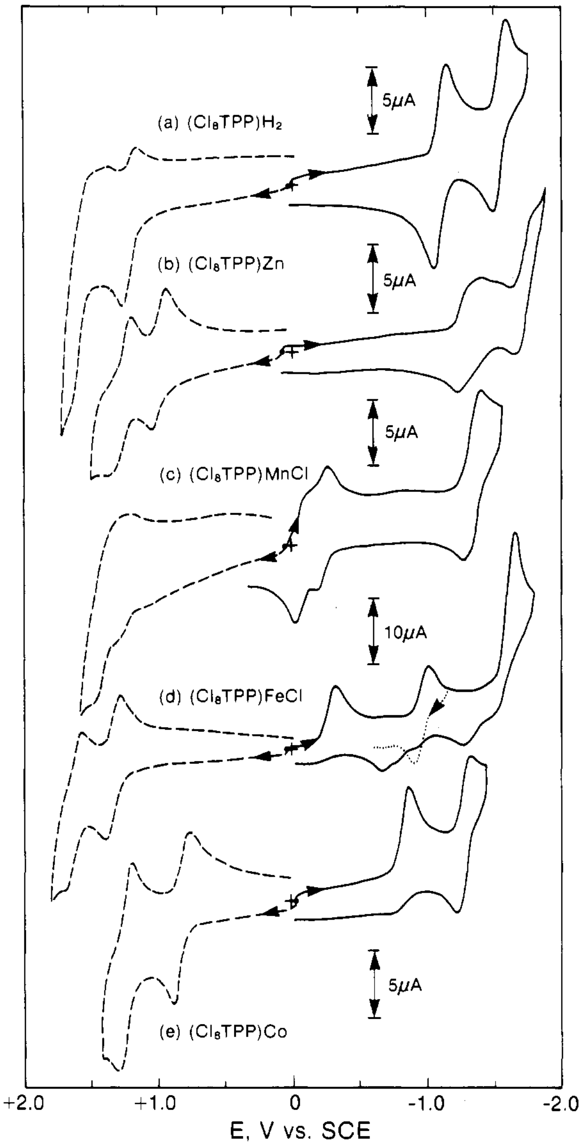

Figure 5. Cyclic voltammograms of 0.5 mM solutions in CH_2Cl_2 [0.1 M $(Bu_4N)ClO_4$]: (a) $(Cl_8TPP)H_2$, (b) $(Cl_8TPP)Zn$; (c) $(Cl_8TPP)Mn(Cl)$; (d) $(Cl_8TPP)Fe(Cl)$; (e) $(Cl_8TPP)Co$. Conditions: scan rate 0.1 V s^{-1}; glassy-carbon working electrode (0.09 cm^2); SCE vs NHE, +0.242 V.

be hybridized to accommodate the molecular orbital geometries and energetics, MnL_3^{3+} (d^5sp; $S = {}^4/_2$), FeL_3^{3+} (d^5sp^2; $S = {}^5/_2$), and CoL_3^{3+} (d^6sp^2; $S = 0$). Oxidation of an aromatic pyridine nitrogen yields a radical cation that can couple with an unpaired metal valence electron (d^6sp^2 in the case of iron) to give a quaternized nitrogen center analogous to that in methylviologen

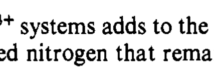

Reduction of $M(bpy)_3^{3+}$ systems adds to the aromatic π-manifold and yields an uncharged nitrogen that remains covalently bound to the metal (again as with methylviologen). The final reduction (Table IIB) yields $[M(bpy)_3]^-$ with the electron delocalized in a bound ligand (analogous to the reduction of free bipyridyl to bpy^-).

Metal Porphyrins. The important (and perhaps most revolutionary) conclusions from the data of Figure 5 and Table IIC are that (a) the redox chemistry for metal porphyrins is ligand-centered and (b) the neutral complexes [M(Por)] consist of uncharged metal centers [($Zn(d^{10}sp)$, $Mn(d^5sp)$, $Fe(d^6sp)$, $Co(d^7sp)$)] bonded via two metal–nitrogen covalent bonds with uncharged porphyrin. Although porphine (H_2Por) is accepted to have two hydrogen atoms bound via covalent bonds to two of its pyrrole nitrogens

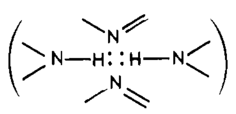

metal porphyrins [M(Por)] are traditionally formulated as metal dications (M^{2+}) complexed via donor bonds of two pyrrole nitrogen anions (Por^{2-}). Reference to Figure 5 indicates that $H_2(Cl_8TPP)$ exhibits two reversible oxidations and two reversible reductions, and there is not any indication of redox chemistry at the two hydrogen atoms. Thus, the removal and addition of electrons is within the π-electron manifold of the porphine ring. The electrochemistry for $Zn(Cl_8TPP)$ closely parallels that for $H_2(Cl_8TPP)$ and appears to involve porphyrin ring electronics and not the zinc valence electrons.

Given (a) the acceptance that the hydrogens of $H_2(Cl_8TPP)$ are covalently bound H atoms and (b) the standard synthesis reaction for zinc–porphyrin (as well as for all uncharged metal–porphyrins) (eq 4), the only reasonable conclusion is that the

$$\underset{(d^{10})}{Zn^{2+}} + H_2(Cl_8TPP) \rightarrow \underset{(d^{10}sp)}{Zn(Cl_8TPP)} + 2H^+ \qquad (4)$$

zinc in $Zn(Cl_8TPP)$ is uncharged with elemental valence electrons ($d^{10}sp$) and bound via two zinc–pyrrole nitrogen sp–p covalent bonds. As such, it is as redox inactive as the hydrogen atoms of $H_2(Cl_8TPP)$. The redox data of Table IIC indicate that the Mn, Fe, and Co also are at the elemental level in their uncharged porphyrins (d^5sp-, d^6sp-, and d^7sp-hybridized valence electrons, respectively). Again, the two reduction couples for each are essentially porphyrin-centered, but the first is facilitated by the partially filled d subshells and the electron affinities of the metal atoms (especially in the case of cobalt, which appears to go to a d^8sp anion upon reduction).

The propensity of transition metals to achieve half-filled d subshells makes $[Fe(Cl_8TPP)](d^6sp)$ subject to the facile removal of a valence electron to give $[Fe^+(Cl_8TPP)](d^5sp)$. Likewise, the oxidation of the porphyrin ring of high-spin ($S = {}^5/_2$) $[Mn(Cl_8TPP)](d^5sp)$ is facilitated by stabilization of the porphyrin cation radical via radical–radical coupling with an unpaired d electron to give a third Mn–N covalent bond.[6] The voltage shift in DMF for this oxidation (−0.16 V) relative to that for the comparable oxidation of $[Zn(Cl_8TPP)](d^{10}sp)$, +1.00 V, is a measure of the covalent Mn–N bond energy [$-\Delta G_{BF} = [(+1.00) - (-0.16)] \times 23.1 = 27$ kcal]. In the case of $Co(Cl_8TPP)$, oxidation also is facilitated by formation of a third Co–N covalent bond with a $-\Delta G_{BF}$ value of 17 kcal. The reductions of $(Cl_8TPP)Fe–Cl$ and $(Cl_8TPP)Fe–OH$, each with d^5sp^2 valence electrons for the iron center, are ligand-centered to give a d^6sp product and the Cl^- and ^-OH ions. The respective oxidation potentials for the free $Cl^-/Cl^\bullet$ and $^-OH/^\bullet OH$ couples in DMF are +2.17 V vs SCE and +0.68 V, which permits an estimate to be made of the Fe–Cl and Fe–OH $-\Delta G_{BF}$ energies. The values are 53 and 32 kcal on the basis of the data in Table IIC.

The present results indicate that the electron-transfer redox reactions of most transition-metal complexes are ligand-centered. This concept is important to an appreciation of the redox character of transition-metal complexes and an understanding of the energetics of their metal–ligand bonds. Electrochemical measurements provide a convenient means to assess the covalent-bond energies. The latter can be used to predict the reactivity of bound ligands (e.g., atomic oxygen, •OH, and •Cl) with substrates. In particular, work is in progress to design effective models for methane monoxygenases, cytochromes P-450, myeloperoxidases, chloroperoxidases, and ligninases.

Acknowledgment. This work was supported under a National Science Foundation Graduate Fellowship (S.A.R.) and a Robert A. Welch Graduate Fellowship (P.K.S.T.). We are grateful to the U.S. Air Force Institute of Technology Civilian Institute Program for the award of a fellowship to S.A.R. The support of the National Science Foundation under Grant No. CHE-8516247 is gratefully acknowledged.